
Article:
Saati, F., Hoppe, K.-A., Marburg, S. et al. (1 more author) (2022) The accuracy of some models to predict the acoustical properties of granular media. Applied Acoustics, 185. 108358. ISSN 0003-682X

https://doi.org/10.1016/j.apacoust.2021.108358

The accuracy of some models to predict the acoustical properties of granular media

Ferina Saati[a,*], Alexander Hoppe[a], Steffen Marburg[a], Kirill V. Horoshenkov[b]

[a] *Vibroacoustics of Vehicles and Machines, Technische Universität München, Boltzmann Str. 15, 85748 Garching, München, Germany*

[b] *Department of Mechanical Engineering, University of Sheffield, Sheffield, S1 3JD, United Kingdom*

Abstract

There is a general lack of understanding on the accuracy of theoretical and empirical models which can be used to predict the acoustical properties of unsaturated granular media. It is also unclear how well these models are suited for parameter inversion in application to these media. In this work three popular prediction models available in commercial software packages, e.g. COMSOL Multiphysics, are used to invert key non-acoustical parameters of two types of glass beads and two fractions of silica sand for which acoustical data are obtained with a standard acoustic impedance tube setup. These results are compared against predictions made with four established non-acoustical analytical models which relate these characteristics to the effective particle size and other pore characteristics. A discrepancy between the two model classes (acoustical and non-acoustical models) and measured data is quantified. This work also quantifies the accuracy of acoustical characterisation methods used to estimate key pore characteristics of granular media with a relatively inexpensive laboratory setup and rapid inversion method based on optimisation.

Keywords: granular, porous, characterisation, inversion, reflection, properties, impedance, acoustical models, non-acoustical models
2018 MSC: 00-01, 99-00

*Corresponding author
Email address: ferina.saati@tum.de (Ferina Saati)

1. Introduction

Characterisation of granular media has been a topic of increasing interest. A range of methods for characterisation are used extensively to predict the behaviour of these media with a series of science and engineering applications including geophysics, sediment acoustics [1] and noise control [2]. The open porosity, defined as the volume fraction of air in the medium, typically in the scope of $0.2 < \phi < 0.6$ is usually way below unity [3]. Several methods exist for characterisation of such materials with the Brunauer-Emmett-Teller (BET) method [4] being one of the most popular. According to [5], characterisation in the specific case of sphere packing is possible through geometrical structure, e.g. using parameters of open porosity or packing fraction. Next to the above parameters, one can also use the pore-size distribution [6], pair-correlation function [7] or structure factor [8]. Revil, Glover, Pezard and Zamora introduced a new permeability prediction equation in an unpublished discussion paper. They used the electrokinetic link between the porous parameters, fluid flow and electrical flow that occurs in a porous medium. The resultant equations were properly described in [9] and this method, which links the viscous permeability, κ_0, characteristic pore length, (denoted by Λ in their work), with the effective grain diameter, d, was consequently called the RGPZ method. The characteristic pore length is usually called viscous characteristic length by the acoustics community.

Allard *et al.* [10] characterise the random packing of glass beads acoustically by measuring macroscopic acoustic parameters. According to Glé *et al.* [2], there has been less than satisfactory acoustic research done in the case of granular media with a particle size distribution and a non-spherical shape. A bulk of existing literature for acoustics of porous media is focused on foams and fibrous absorbers, which have porosity of close to unity. Very few

other papers report the application of the Allard *et al* approach [10] to granular media. The work by Fellah *et al* [11] used 60-420 kHz ultrasound in combination with the time-domain version of the Allard *et al* model to estimate some non-acoustical parameters of sand with grain size below 500 μm. However, this work did not present any comparison between the modelled and predicted acoustical properties in the audible frequency range which is typical for the use in an impedance tube, i.e. 100 - 6000 Hz. As a result, the relations between the particle size distribution and acoustical properties of this class of porous (granular) materials are still not well understood particularly in the frequency range that is covered by a standard impedance tube setup.

Describing a granular medium at a macroscopic scale can be done by evaluating several macroscopic parameters that depend solely on the geometry of the granular structure [12], some of which can be assessed from acoustical estimations. The choice of the characterisation model is critical because the more complicated a model is, the more input parameters are required to fit data obtained from more than one type of measurement. The rank of the design vector increases with a rising number of parameters. This leads to ambiguity in the inverted parameter values [13]. To fix this problem, usage of a constrained optimisation (functional minimisation) method is common. The open porosity ϕ and viscous permeability, κ_0, [10] or so-called air flow resistivity, $\sigma = \eta/\kappa_0$, (η being the dynamic viscosity of saturating fluid Nsm^{-2}) are routinely measurable using non-acoustical techniques, whereas other parameters such as the tortuosity α_∞ and viscous characteristic length Λ are more difficult to accurately measure non-acoustically.

In air-saturated granular media, wave propagation occurs mainly in the saturating fluid because there is a large density contrast. As a result, the motionless structure assumption is

usually made [14] and equivalent-fluid models for the oscillatory behaviour of the saturating fluid under acoustic excitation are usually used [15]. In these models, the dynamic tortuosity of the equivalent fluid is given by Johnson *et al.* [16] to account for viscous and inertia effects, whereas the dynamic compressibility of the equivalent fluid is given by Allard and Atalla [17] to account for thermal effects. The work by Fellah *et al.* [12] suggests a simple method for measuring porosity and tortuosity for air-saturated granular media such as glass beads. Intuitively, one can suggest that the pore size distribution and porosity are key parameters which determine the acoustical properties of granular media. A simple way to describe the pore size distribution in an acoustical model is to make use of the median pore size $\bar{s}$ and the standard deviation in pore size σ_s as suggested recently by Horoshenkov *et al.* [18]. Combined with the porosity, this model should be applicable to all sorts of porous materials including granular media. It is now of interest to better understand how this model would work in comparison with more complicated models for the inversion of key non-acoustical parameters of granular media from acoustical data obtained with a standard laboratory setup.

Therefore, this paper is focused on the ability of several popular models for the acoustical properties of granular media to invert key non-acoustical pore characteristics from impedance tube data. More specifically, this paper studies the accuracy of the parameter inversion using the methods of Johnson-Champoux-Allard-Lafarge *et al.* [16, 19], Miki [20] and the more recent non-uniform pore size distribution [21] model by Horoshenkov *et al.* [18]. These models are now incorporated in a number of standard software packages including COMSOL Multiphysics® and AlphaCell. The parameters resulting from the inversion are compared to results from non-acoustical models of Umnova *et al.* [22], Berryman [23], Revil, Glover,

Pezard and Zamora (RGPZ) [9] and Kozeny and Carman [24] which relate key properties of granular media with the grain size. To the best of our knowledge, this work has never been done systematically and it is a main novelty of our paper. In this paper, we compare the pore parameters of granular media predicted with non-acoustical methods against those inverted with acoustical methods. The paper is organised as follows. Section 2 introduces the aforementioned models. Section 3 gives a summary of inversion techniques used together with the acoustical prediction method and presents the impedance tube measurement set-up. The results, error analysis and final remarks are found in sections 4 and 5, respectively.

2. Models for the non-acoustical and acoustical properties of porous media

Among the 13 parameters required by the full Biot model [14] the prediction of elastic wave propagation in a majority of types of unconsolidated, rigid frame granular media, 4 pore parameters are of particular interest: the open porosity, ϕ; tortuosity α_∞; viscous permeability, κ_0; and some measure of the effective pore size, s, and its distribution.

2.1. Analytical models

There are a number of models that can relate to some of the above pore parameters. The work by Berryman [23] suggests that the tortuosity of a stack of identical, spherical solid particles can be expressed via porosity only:

$$\alpha_\infty = 1 - b(1 - 1/\phi), \tag{1}$$

in which b depends on the particle shape, e.g. $b = 1/2$ for spherical grain packing and $0<b<1$ for other shapes. Alternative values for b were introduced for spherical or uniform cylindrical

shapes by [25] and [26], respectively. The above equation suggests that the tortuosity for this type of material is basically independent of the effective pore size, but depends on the way particles are arranged in the stack.

If the porosity, tortuosity and particle radius R are known, then a characteristic measure of the pore size in a stack of spherical particles can be predicted using the equation suggested by Umnova *et al.* [22]:

$$\Lambda = \frac{4(1-\Theta)\phi\alpha_\infty}{9(1-\phi)}R. \tag{2}$$

In the above equation, Λ is the characteristic viscous length of the pore and Θ is the ratio of particle to equivalent cell volume [22]:

$$\Theta = 0.675(1-\phi) \tag{3}$$

given for the case of cubic packaging of spheres. The permeability of this medium is [22]:

$$\kappa_0 = \frac{\phi^2 d_{\text{eff}}^2}{18(1-\phi)(1-\Theta)\Omega_k}, \tag{4}$$

where $\Omega_k = 5(5 - 9\Theta_k^{1/3} + 5\Theta_k - \Theta_k)^{-1}$ and $d_{\text{eff}} = 2R$ is the effective mean diameter of the particles. Umnova *et al.* also proposed an equation for the tortuosity which is an alternative to Eq. (1):

$$\alpha_\infty = 1 + \frac{(1+2\Theta)(1-\phi)}{2\phi}. \tag{5}$$

In order to determine the viscous permeability, κ_0, the Kozeny-Carman model [24] can

also be used. It expresses the permeability of a stack of pseudo-spherical particles as:

$$\kappa_0 = \frac{\phi^3}{180(1-\phi)^2} d_{\text{eff}}^2. \tag{6}$$

The Revil, Glover, Pezard and Zamora (RGPZ) model [9] suggests the following equation for the viscous characteristic length[1]:

$$\Lambda = \frac{\sqrt{3} d_{\text{eff}}}{2m(F-1)}, \tag{7}$$

from which the permeability is derived through the following formula (RGPZ model, Eq. (12) in [28]):

$$\kappa_0 = \frac{d_{\text{eff}}^2}{4am^2} \phi^{3m}, \tag{8}$$

where m is the cementation exponent, dependent on the shape of the particles and the porosity, increasing as they become less spherical. The parameter a is a pore shape factor which accounts for a wide range of pore geometries. In this study, we consider $a = 8/3$ based on [9].

In acoustics, it is more common to deal with the flow resistivity rather than with the permeability which is defined as:

$$\sigma = \frac{\eta}{\kappa_0}, \tag{9}$$

[1]Here we refer to the viscous characteristic length which is used in the Johnson-Champoux-Allard-Lafarge model [27]. There are some differences between the characteristic lengths defined by Johnson *et al.* [16], Λ, and Revil, Glover, Pezard and Zamora [28], Λ^2_{RGPZ}. The viscous characteristic lengths defined by Johnson is $\Lambda^2 = 3\Lambda^2_{RGPZ}$. In the case of uniform glass beads or other types of pseudo-spherical particles with the pore shape factor of $a = 8/3$, there appears a $\sqrt{3}$ factor in Eq. (7)

where $\eta = 1.81 \times 10^{-5}\,\mathrm{Pa\,s}$ is the dynamic viscosity of air at ambient temperature.

2.2. The Miki model

There are a number of empirical models which use some of the above non-acoustical parameters to predict the acoustical properties of porous media. Miki [20] suggested an empirical three-parameter model which has become very popular because of the limited number of input parameters it requires. According to this model, the characteristic impedance of a porous medium can be calculated from:

$$\tilde{Z}_c(f) = \frac{\alpha_\infty^{0.5}}{\phi}\left[1 + 0.070\left(\frac{f}{\sigma}\right)^{-0.632}\right] - \mathrm{i}0.107\frac{\alpha_\infty^{0.5}}{\phi}\left(\frac{f}{\sigma}\right)^{-0.632}, \tag{10}$$

where f is the frequency of sound and $\tilde{Z}_c(f)$ is the characteristic impedance of the porous medium normalized with respect to the impedance of air. The wavenumber is given by:

$$\tilde{k}(f) = \frac{2\pi f \alpha_\infty^{0.5}}{c_0}\left[1 + 0.109\left(\frac{f}{\sigma}\right)^{-0.618} + 0.16\mathrm{i}\left(\frac{f}{\sigma}\right)^{-0.618}\right], \tag{11}$$

where c_0 is the sound speed in air.

2.3. Non-uniform pore size distribution model

Horoshenkov *et al.* [18] showed theoretically that the acoustical properties of materials with a pore size distribution can be predicted from the knowledge of the porosity, median pore size and standard deviation in pore size. They use Padé approximations to express the complex compressibility $\tilde{C}(\omega)$ and dynamic density $\tilde{\rho}(\omega)$ of the effective fluid in a material with non-uniform pores of which the radius is distributed log-normally ($\omega = 2\pi f$ being the angular frequency). The choice of log-normal distribution is supported by the fact that a

majority of pore size distribution in granular media found in geophysics and outdoor sound propagation problems [29] obeys the log-normal law [30]. In this non-uniform pore size distribution model (NUPSD) the dynamic density is averaged over all possible pore sizes and approximated with [18]:

$$\frac{\tilde{\rho}(\omega)}{\rho_0} \simeq \frac{\alpha_\infty}{\phi}\left(1+\epsilon_\rho^{-2}\tilde{F}_\rho(\epsilon_\rho)\right), \tag{12}$$

where

$$\tilde{F}_\rho(\epsilon_\rho) = \frac{1+\theta_{\rho,3}\epsilon_\rho+\theta_{\rho,1}\epsilon_\rho^2}{1+\theta_{\rho,3}\epsilon_\rho} \tag{13}$$

is the Padé approximant to the viscosity correction function with $\epsilon_\rho = \sqrt{\frac{-\mathrm{i}\omega\rho_0\alpha_\infty}{\phi\sigma}}$, $\theta_{\rho,1} = 1/3$, $\theta_{\rho,2} = e^{-1/2(\sigma_s \log 2)^2}/\sqrt{2}$ and $\theta_{\rho,3} = \theta_{\rho,1}/\theta_{\rho,2}$. In these equations, σ_s is the standard deviation in the pore size and ρ_0 is the rest density of air in the pores (kgm^{-3}).

The bulk flow resistivity of the porous medium is:

$$\sigma = \frac{8\eta\alpha_\infty}{\bar{s}^2\phi}e^{6(\sigma_s \log 2)^2}. \tag{14}$$

The bulk complex compressibility of the fluid in the material pores is:

$$\tilde{C}(\omega) = \frac{\phi}{\gamma P_0}\left(\gamma - \frac{\gamma-1}{1+\epsilon_c^{-2}\tilde{F}_c(\epsilon_c)}\right), \tag{15}$$

where

$$\tilde{F}_c(\epsilon_c) = \frac{1+\theta_{c,3}\epsilon_c+\theta_{c,1}\epsilon_c^2}{1+\theta_{c,3}\epsilon_c}. \tag{16}$$

In the above two equations, $\epsilon_c = \sqrt{\frac{-\mathrm{i}\omega\rho_0 N_{Pr}\alpha_\infty}{\phi\sigma^{'}}}$, $\theta_{c,1} = \theta_{\rho,1} = 1/3$, $\theta_{c,2} = e^{3/2(\sigma_s \log 2)^2}/\sqrt{2}$, $\theta_{c,3} = \theta_{c,1}/\theta_{c,2}$. $\gamma = 1.4$ is the ratio of specific heats, $N_{Pr} = 0.71$ is the Prandtl number and $P_0 = 101320$ Pa is the ambient atmospheric pressure taken at 20^oC. The thermal flow resistivity is defined as:

$$\sigma^{'} = \frac{8\eta\alpha_\infty}{\bar{s}^2\phi} e^{-6(\sigma_s \log 2)^2}. \tag{17}$$

In their work [18], it has been shown that the tortuosity is not an independent parameter, but can be expressed via the standard deviation in log-normal pore size distribution:

$$\alpha_\infty = e^{4(\sigma_s \log 2)^2}. \tag{18}$$

The work [18] has also shown that the two characteristic lengths in the JCAL model [19] are not independent parameters and can be expressed as functions of the median pore size and standard deviation in the pore size:

$$\Lambda = \bar{s} e^{-5/2(\sigma_s \log 2)^2}, \tag{19}$$

$$\Lambda^{'} = \bar{s} e^{3/2(\sigma_s \log 2)^2}. \tag{20}$$

Effectively, the model proposed in [18] is a 3-parameter model which depends only on the porosity, ϕ, median pore size, $\bar{s}$ and the standard deviation in pore size, σ_s. These parameters are directly measurable with non-acoustical methods.

2.4. Johnson-Champoux-Allard-Lafarge model

The Johnson-Champoux-Allard-Lafarge (JCAL) [19] is a very popular model which can predict the acoustical properties of porous media from the knowledge of 6 non-acoustical parameters: the porosity, ϕ, viscous flow resistivity, σ, tortuosity, α_∞, viscous characteristic length, Λ, thermal characteristic length, Λ' and static thermal permeability k_0' or its counterpart, the thermal flow resistivity, $\sigma' = \eta/k_0'$. In the JCAL model, the dynamic density and dynamic compressibility are predicted from [17]:

$$\tilde{\rho}(\omega) = \frac{\rho_0 \alpha_\infty}{\phi}\left(1 + \frac{\phi\sigma}{i\omega\rho_0\alpha_\infty}\sqrt{1 + \mathrm{i}\frac{4\omega\rho_0\eta\alpha_\infty^2}{\sigma^2\phi^2\Lambda^2}}\right), \tag{21}$$

and

$$\tilde{C}(\omega) = \frac{\phi}{\gamma P_0}\left[\gamma - \frac{\gamma - 1}{1 - \frac{i\sigma'\phi}{\rho_0\alpha_\infty N_{Pr}\omega}\left(1 + \frac{4i\alpha_\infty^2\eta\rho_0 N_{Pr}\omega}{(\sigma'\Lambda'\phi)^2}\right)^{1/2}}\right], \tag{22}$$

respectively. The above equations for the dynamic density and bulk modulus are used to predict the characteristic impedance:

$$\tilde{Z}_c = \sqrt{\tilde{\rho}\tilde{C}}, \tag{23}$$

and the complex wavenumber:

$$\tilde{k} = \omega\sqrt{\tilde{\rho}/\tilde{C}}. \tag{24}$$

A majority of porous materials are presented and measured in the form of a hard-backed layer of a finite thickness h. Therefore, the acoustic surface impedance of this layer is given

as:

$$Z_s = \tilde{Z}_c \coth(-\mathrm{i}\tilde{k}h). \tag{25}$$

In the above equation, the functions $\tilde{Z}_c$ and $\tilde{k}$ can be predicted using either of the three models presented above.

3. Inverse Characterisation Techniques and Laboratory Experiments

While open porosity ϕ and flow resistivity σ are directly measurable using standard techniques, other parameters such as tortuosity α_∞ or characteristic lengths Λ and Λ' have obscure physical meaning and require expensive setups and experienced experimentalists [31]. In this work, we apply inverse characterisation to determine key non-acoustical parameters from acoustical data for several air-saturated granular media. This work makes use of a standard acoustical impedance tube which is loaded with a hard-backed porous sample with thickness h as shown in Fig. 1 and ISO 10534-2 method detailed in Ref. [32]. The standard ISO 10534-2 method enables us to measure directly the complex, normal incidence reflection coefficient, $r(\omega)$ from which the normal incidence surface impedance, $Z_s(\omega)$ of the hard-backed layer is calculated from:

$$Z_s = \frac{1+r}{1-r}. \tag{26}$$

115

In this study, the Nelder-Mead optimisation technique [3] is used to minimise the following cost function:

$$\boldsymbol{F}(\boldsymbol{x}) = \frac{1}{N}\sum_{n=1}^{N} |r_n^p(\boldsymbol{x}) - r_n^m|, \tag{27}$$

where superscripts p and m represent predicted and measured complex reflection coefficient,

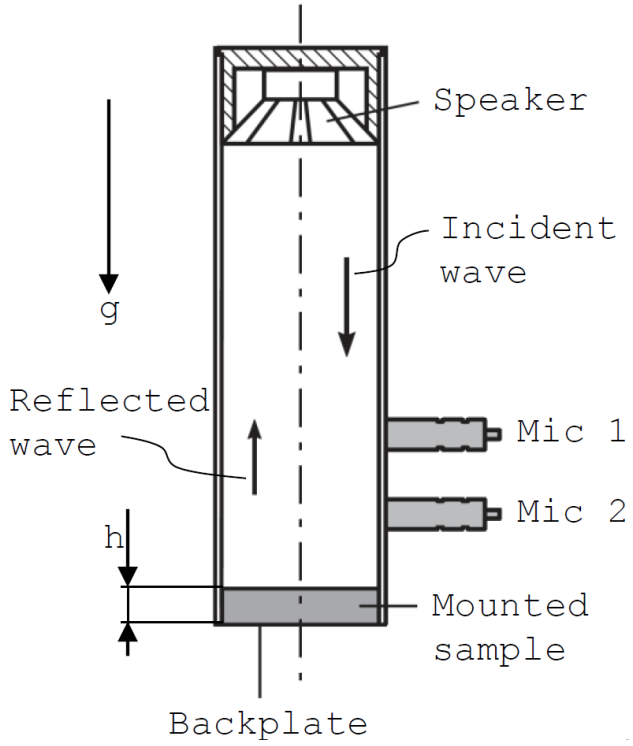

Figure 1: Schematic of the acoustical impedance tube setup used in the reported experiments.

respectively. N is the total number of frequencies at which the reflection coefficient has been measured. Minimising the cost function is a practical way to find the optimal parameter vector $\boldsymbol{x}$ for which the function $\boldsymbol{F}$ has a clear minimum, i.e. the difference between the measured and predicted reflection coefficient is smallest. To find the best fit, it is necessary to look for the global minimum of the cost function. The composition of the parameter vector $\boldsymbol{x}$ in Eq. (27) depends on the choice of the model to predict $r_n^p(\boldsymbol{x})$. The parameter vector in the case of the JCAL model [10] is $\boldsymbol{x} = \{\phi, \sigma, \sigma', \alpha_\infty, \Lambda, \Lambda'\}$. In the case of the Miki model [20], it is $\boldsymbol{x} = \{\phi, \sigma, \alpha_\infty\}$. In the case of the Padé approximation model [18], it is $\boldsymbol{x} = \{\phi, \bar{s}, \sigma_s\}$.

All measurements described in this section were performed in the Jonas Laboratory at the University of Sheffield on four samples of uniform glass beads and silica sands. The impedance tube used for these experiments is depicted schematically in Figure 1. It was a vertically oriented, 45 mm diameter impedance tube manufactured by Materiacustica. It is set up to work in the frequency range of 50 - 4180 Hz with the frequency resolution of 12.5 Hz. 1 second exponential sine sweep was used repeatedly together with deconvolution to calculate the impulse response of the tube and cross-spectral functions required by the ISO10534-2 method [32]. The tube was mounted in a vertical manner in order to fill the volume of the sample holder uniformly and flatten the sample's top surface. Figure 2 provides two photographs of the 5 mm diameter glass beads (left) and 1.8 mm diameter silica sand (right) filling the sample holder.

Bulk density ρ was calculated by dividing the mass of the material sample by its volume fit in the sample holder in the impedance tube. The mass of each sample was measured with a Kern KB10000-1 N scale. The open porosity was calculated from grain density and bulk

Figure 2: Photographs of selected granular materials in the impedance tube sample holder. Top - 5 mm diameter glass beads. Bottom - 1.8 mm diameter silica sand.

material density data using the following equation:

$$\phi = 1 - \frac{\rho}{\rho_p}. \tag{28}$$

The flow resistivitiy σ was measured non-acoustically using AFD AcoustiFlow 300 manufactured by Akustik Forschung Dresden. Each sample was directly tested via AFD 311 software package. The measurement was done in accordance with the ISO 9053 [33] using a direct airflow method. A 30 mm thick sample of each granular material was placed in the sample holder on a wire mesh and its flow resistivity was measured at a temperature of 20.0 ± 0.5°C.

In the case of glass beads, the equivalent particle diameter was measured with a caliper. In the case of silica sands, this parameter was taken as a median from the sieve analysis provided by David Ball Specialist Sands Group. Table 1 lists the materials types used in this study and their values of density, porosity, characteristic particle diameter and air flow resistivity measured non-acoustically. Sample 1 and Sample 2 refer to glass beads of 2 and 5 mm bead diameter, respectively. Sample 3 and Sample 4 refer to silica sands of fraction A and B, respectively. Standard deviation of the air flow resistivity is listed as σ_σ in this table. The accuracy of other parameters listed in Table 1 was within 3 decimal places, i.e.$\pm$ 0.5%.

The surface impedance of these material specimens was measured according to the ISO 10534-2 [32]. The constraint minimisation problem (Eq. (27)) was solved with the standard MATLAB minimisation subroutine 'fminsearchbnd()'. In this analysis, the frequency range of interest, or the constraints of the function was set to 200 - 3500 Hz. Below the lower frequency limit, the signal-to-noise ratio was relatively low. Above the higher frequency

Table 1: A summary of porous sample properties measured non-acoustically

Material type	**Sample 1**	**Sample 2**	**Sample 3**	**Sample 4**
ρ_p [kg m^{-3}]	2500	2500	2650	2650
ρ [kg m^{-3}]	1608	1580	1588	1635
ϕ	0.36	0.37	0.40	0.38
d_{eff} [mm]	2.10	5.02	1.77	0.89
σ [Pa s m^{-2}]	7287 $\pm$ 64	1752 $\pm$ 35	10944 $\pm$ 129	35379 $\pm$ 137

limit, it was difficult to maintain a good phase match between the two microphones in the impedance tube. The bounds in the minimization problem (eq. (27)) were set as following: (i) $10^{-6} < \bar{s}, \Lambda, \Lambda' < 10^{-2}$ m; (ii) $0.1 < \phi < 1$; (iii) $0 < \sigma_s < 1$; (iv) $1 < \alpha_\infty < 10$; (v) $10^2 < \sigma < 10^8$ Pa s m^{-2}.

The sample holder thickness was set to $h = 80\,\text{mm}$ for all the experiments. Each sample was placed in the holder and shaken until its height was matched with the height of sample holder. This process and subsequent measurements were repeated at least three times for the purpose of averaging. The reproducibility of this experiment was within 2% of deviations from each other. The measured reflection coefficient data for the four materials and Matlab code to invert the non-acoustical parameters using the three prediction models can be found here [34].

4. Results

The reflection coefficient data were used to invert the key non-acoustical parameters for the pore size distribution (NUPSD), Johnson-Champoux-Allard-Lafarge (JCAL) and the Miki models. Figures 3 and 4 present a comparison between the measured and predicted complex reflection coefficient for Samples 1-4. This inversion process was repeated on every

set of measured data in the frequency range in which the upper limit was progressively changed from 1000 to 3500 Hz in 500 Hz steps. This was done to understand the variation in the values of key non-acoustical parameters inverted through this minimisation process. This variability is reflected in the standard deviation which accompanies the parameter values inverted with the three models. These data are presented in Tables 2-5.

The quality of the fit between the measured and predicted reflection coefficient spectra was estimated from the relative error as

$$\varepsilon = \sum_{n=1}^{N} |r_n^p(\boldsymbol{x}) - r_n^m| / \sum_{n=1}^{N} |r_n^m|. \tag{29}$$

It was noted that the relative error between the measured data and prediction progressively increased from 2-5% to 25-33% with the increased upper frequency limit. The greater errors were observed in the case of silica sands. These were likely to relate to a broader distribution in the particle size. This distribution could have led to some stratification in the material pore structure when the sample was shaken in the sample holder to be compacted to a settled value of density.

Tables 2 - 5 also list the parameter values predicted with the analytical models detailed in section 2. In these tables, the Revil, Glover, Pezard and Zamora model is referred to as RGPZ and the Kozeny and Carman model as KC models. The other analytical models carry the first author's name. The measured values of the viscous characteristic lengths quoted in these tables for 2 and 5 mm glass beads were taken from Table 1 in Ref. [35]. These values were measured independently using the mercury injection capillary pressure method. The measured values of the thermal characteristic lengths for glass beads shown in these tables

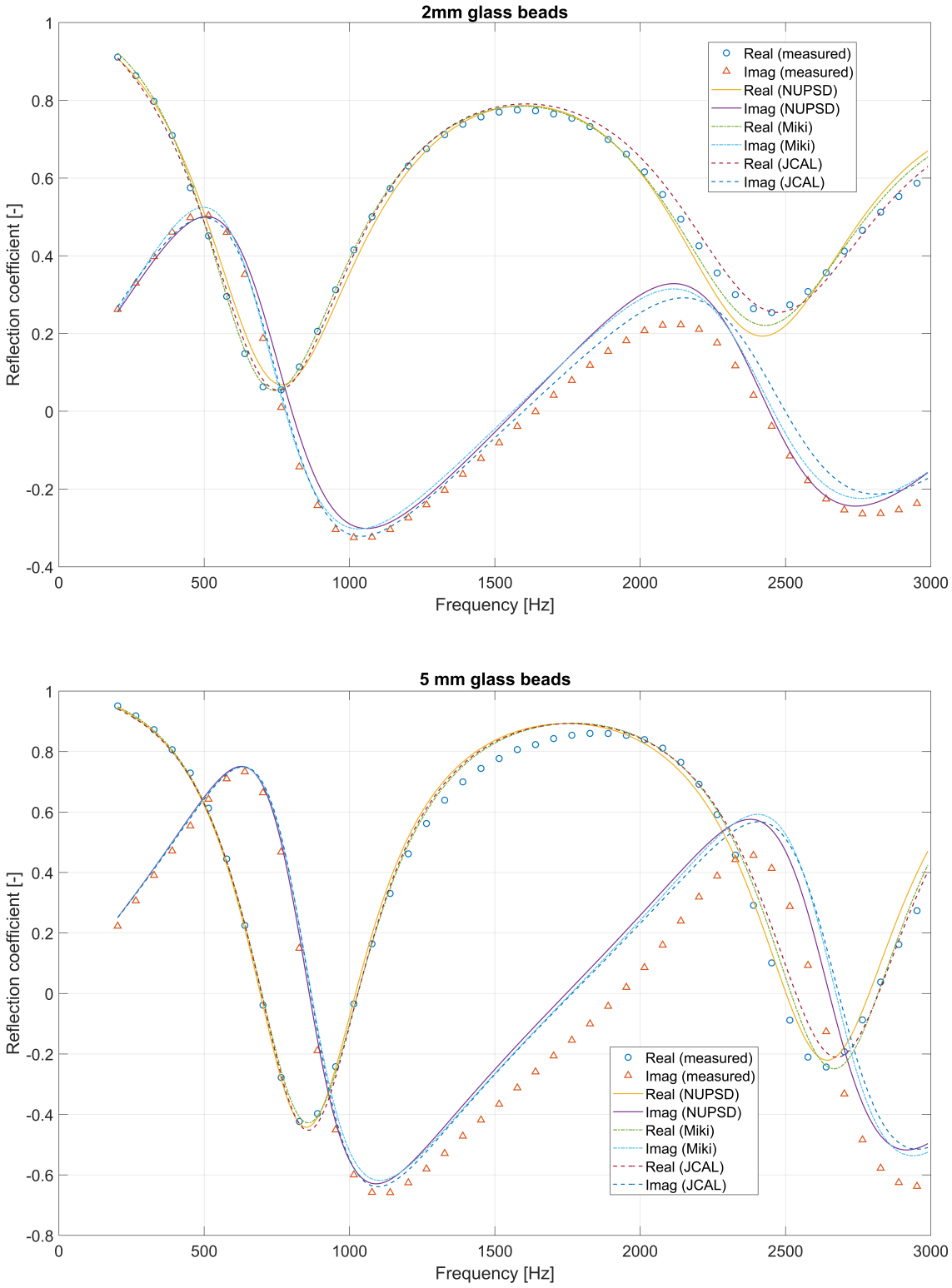

Figure 3: A comparison between the measured and predicted spectra of the complex reflection coefficient for glass beads.

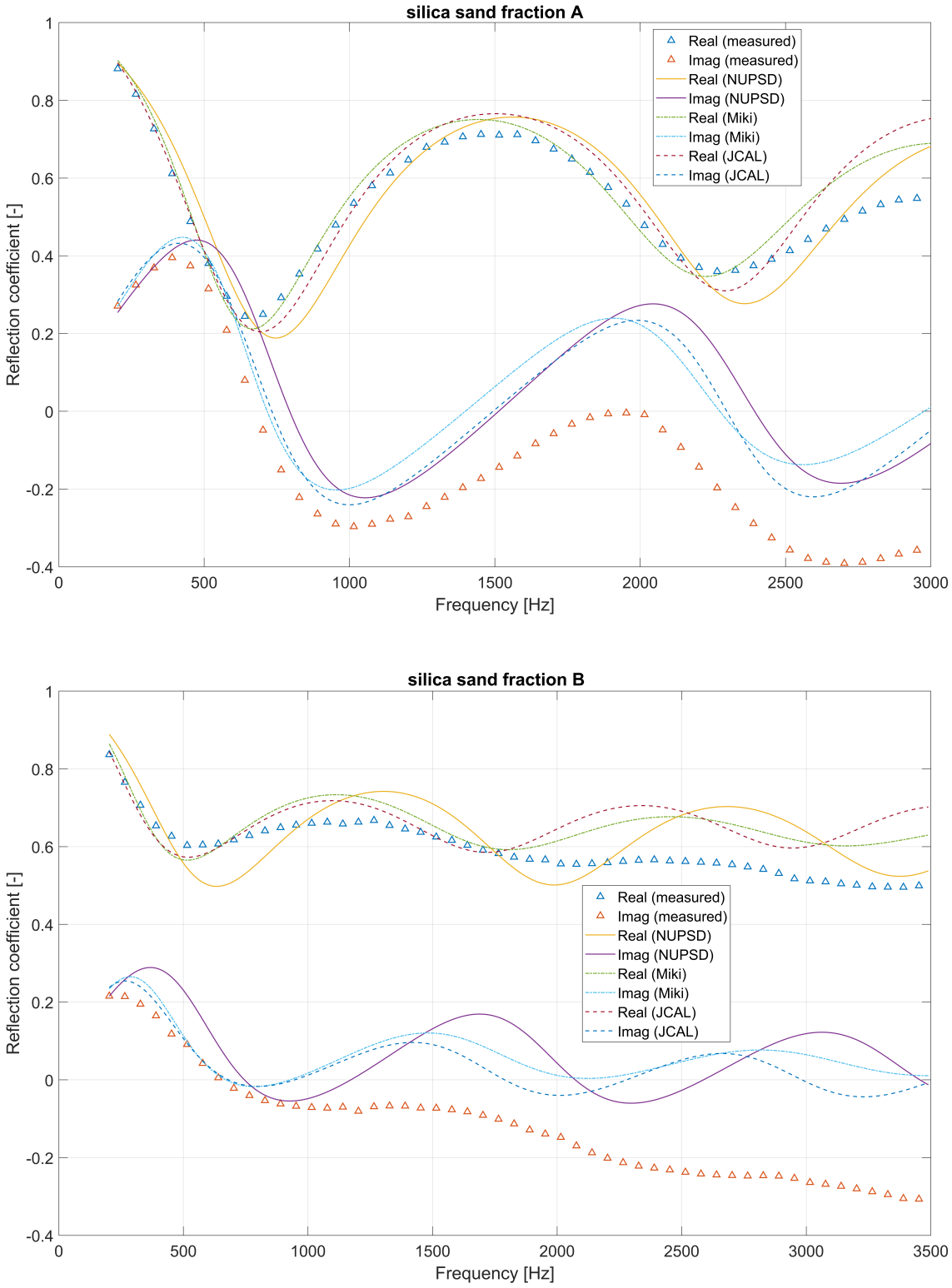

Figure 4: A comparison between the measured and predicted spectra of the complex reflection coefficient for silica sands

were extrapolated from data obtained by Leclaire *et al.* for 1.64 mm diameter glass beads from an independent water suction experiment [36]. The value of the cementation exponent used with the RGPZ model (see section 2) was set to $m = 1.49$ in the case of 2 mm glass beads, $m = 1.57$ in the case of 5 mm glass beads (Table 1 in [35]) and $m = 1.8$ in the case of silica sands [2]. It was impossible to find measured data for the tortuosity, thermal flow resistivity and mean pore size for these four materials. Therefore, the inverted or directly predicted values for these parameters are provided for future reference and not discussed against any data.

4.1. Sample 1: 2 mm *glass beads*

The top part of Figure 3 presents an example of the comparison between the measured and predicted spectra for the complex reflection coefficient of an 80 mm hard-backed layer of 2 mm glass beads. Generally, there is a close agreement between the predicted and measured reflection coefficient spectra. Table 2 presents a summary of the non-acoustical parameters which were inverted using the three models for the acoustical properties of porous media and analytical models detailed in section 2. The results suggest that any of the three models can invert the value of porosity with an error of less than 10%. The JCAL model is the most accurate in terms of the inverted porosity value (1.5%) when compared against the measured value.

In terms of the inverted tortuosity values, the three models agree within 9.5%. The mean value of the inverted tortuosity is $\bar{\alpha}_\infty = 1.33$. This value is rather different from that predicted by Berryman's ($\alpha_\infty = 1.85$) or Umnova's ($\alpha_\infty = 2.66$) models. There is no

[2] Private correspondence with Prof. P. W. J. Glover

Table 2: A summary of the values of non-acoustical parameters for Sample 1 (glass beads of 2 mm diameter) measured, inverted acoustically and predicted non-acoustically.

Model	ϕ	α_∞	σ Pa s m^{-2}	σ' Pa s m^{-2}	$\bar{s}$ μm	$\sigma_{\bar{s}}$ φ-units	Λ μm	Λ' μm
Measured	0.360	-	7290	-	-	0.27	253	321
	-	-	$\pm$64	-	-	-	-	-
NUPSD	0.393	1.52	8690	2490	349	0.47	269	409
	$\pm$0.007	$\pm$0.06	$\pm$264	$\pm$340	$\pm$18	$\pm$0.02	$\pm$7	$\pm$27
JCAL	0.355	1.34	5550	5550	-	-	231	311
	$\pm$0.005	$\pm$0.05	$\pm$670	$\pm$670	-	-	$\pm$27	$\pm$171
Miki	0.388	1.50	5680	-	-	-	-	-
	$\pm$0.002	$\pm$0.02	$\pm$157	-	-	-	-	-
Umnova	-	2.66	6730	-	-	-	377	-
Berryman	-	1.89	-	-	-	-	-	-
RGPZ	-	-	10312	-	-	-	324	-
Kozeny & Carman (KC)	-	-	7150	-	-	-	-	-

measured tortuosity value to compare against.

The flow resistivity inverted with the three models is accurate within 31%. The NUPSD model is most accurate in terms of the inverted flow resistivity value (overestimates by 16%). This estimate is close to the value estimated for the same granular medium by Horoshenkov *et al.* (Table 1 [18]). In terms of the directly predicted flow resistivity value, the KC model is very accurate within 2%. Umnova's model underestimates the measured flow resistivity by 8% and the RGPZ overestimates it by 29%.

The NUPSD overestimates significantly (by 74%) the standard deviation in the pore size distribution. It is also 18% higher than that quoted in [18] for the same type of granular medium. However, the measured value for this parameter was taken for glass beads of a smaller size and at a different compaction state ($d_{\text{eff}} = 1.64$,mm and $\phi = 0.335$ in [37]). Therefore, this comparison is not exactly direct. On the other hand, the NUPSD and the

JCAL model invert the viscous characteristic length rather accurately within 9%. The value of the thermal characteristic length inverted with the JCAL model is accurate within 3% which is impressive. Because of the relation (20) and higher than expected value of the standard deviation, the NUPSD model overestimates the thermal characteristic length by 22%. The standard deviation in the pore size estimated in this work is $\sigma_s = 0.47$, which is larger than $\sigma_s = 0.388$ estimated in [18] and $\sigma_s = 0.27$ measured in [36]. We also note that the thermal characteristic length for this medium was extrapolated from independently obtained data for silica sand with a different particle diameter of $d_{\text{eff}} = 1.64$, mm but similar porosity $\phi = 0.37$ [36].

4.2. Sample 2: 5 mm *glass beads*

The bottom part of Figure 3 presents an example of the comparison between the measured and predicted spectra for the complex reflection coefficient of an 80 mm hard-backed layer of 5 mm glass beads. Generally, there is a close agreement between the predicted and measured real part of the reflection coefficient spectra. The agreement between the predicted and measured imaginary parts becomes less close as the frequency of sound increases above 1000 Hz. Table 3 presents a summary of the non-acoustical parameters which were inverted using the three models for the acoustical properties of porous media and analytical models detailed in section 2. The inverted porosity values are accurate within 5%. The Johnson-Champoux-Allard-Lafarge model is the most accurate in terms of the inverted porosity value (1%) when compared against the measured value. NUPSD overestimates the porosity by 5%. The pattern in the inverted and predicted tortuosity values for this granular medium is similar to that described for the case of 2 mm glass beads.

Table 3: A summary of the values of non-acoustical parameters for Sample 2 (glass beads of 5 mm diameter) measured, inverted acoustically and predicted non-acoustically.

Model	ϕ	α_∞	σ Pa s m^{-2}	σ' Pa s m^{-2}	$\bar{s}$ μm	$\sigma_{\bar{s}}$ φ-units	Λ μm	Λ' μm
Measured	0.370	-	1750	-	-	0.27	476	803
	-	-	$\pm$ 35	-	-	-	-	-
NUPSD	0.388	1.32	1817	789	645	0.38	542	716
	$\pm$0.007	$\pm$0.03	$\pm$77	$\pm$67	$\pm$24	$\pm$0.01	$\pm$14	$\pm$32
JCAL	0.382	1.31	1023	-	-	-	615	644
	$\pm$0.009	$\pm$0.05	$\pm$767	$\pm$664	-	-	$\pm$73	$\pm$102
Miki	0.395	1.37	1149	-	-	-	-	-
	$\pm$0.007	$\pm$0.03	$\pm$64	-	-	-	-	-
Umnova	-	2.58	971	-	-	-	966	-
Berryman	-	1.85	-	-	-	-	-	-
RGPZ	-	-	2060	-	-	-	733	-
KC	-	-	1021	-	-	-	-	-

There are significant differences in the values of the flow resistivity inverted with the three models. The NUPSD model is the most accurate predicting the flow resistivity within 3.6% from the measured value. The JCAL and the Miki models significantly underestimate the flow resistivity by 71% and 52%, respectively. Umnova's model also underpredicts the flow resistivity by 80%, so does the KC model (71%). On the other hand, the RGPZ model is relatively accurate and slightly overpredicts the flow resistivity of this medium by 15%.

All the models underestimate the measured value of the viscous characteristic length. The NUPSD model provides the most accurate estimate for this parameter being accurate within 12%. Umnova's model is the least accurate predicting a value 50% higher. The value of the thermal characteristic length inverted with the NUPSD model is a 12% underestimate. The JCAL model underestimates this value by 25%.

Table 4: A summary of the values of non-acoustical parameters for Sample 3 (silica sand fraction A) measured, inverted acoustically and predicted non-acoustically.

Model	ϕ	α_∞	σ Pa s m^{-2}	σ' Pa s m^{-2}	$\bar{s}$ μm	$\sigma_{\bar{s}}$ φ-units	Λ μm	Λ' μm
Measured	0.40	-	10900	-	-	-	-	-
	-	-	$\pm$129	-	-	-	-	-
NUPSD	0.420	1.77	13440	2560	329	0.54	230	409
	$\pm$0.015	$\pm$0.2	$\pm$563	$\pm$1282	$\pm$38	$\pm$0.07	$\pm$11	$\pm$61
JCAL	0.363	1.91	11610	10580	-	-	12510	75310
	$\pm$0.008	$\pm$0.3	$\pm$2214	$\pm$3140	-	-	$\pm$8763	$\pm$6202
Miki	0.399	1.70	9300	-	-	-	-	-
	$\pm$0.004	$\pm$0.1	$\pm$506	-	-	-	-	-
Umnova	-	2.36	5740	-	-	-	368	-
Berryman	-	1.75	-	-	-	-	-	-
RGPZ	-	-	28100	-	-	-	203	-
KC	-	-	5850	-	-	-	-	-

4.3. Sample 3: silica sand fraction A

The top part of Figure 4 presents an example of the comparison between the measured and predicted spectra for the complex reflection coefficient of an 80 mm hard-backed layer of silica sand fraction A. Generally, there is a close agreement between the predicted and measured real part of the reflection coefficient spectra. The agreement between the predicted and measured imaginary parts is relatively poor. Table 4 presents a summary of the non-acoustical parameters which were inverted using the three models for the acoustical properties of porous media and analytical models detailed in section 2.

The three models for the acoustical properties of porous media allow for an inversion of the porosity for this sand with an accuracy of 10%. The Miki model provides the most accurate estimate close to the measured value within 0.1%. The tortuosity estimate obtained with Berryman's model is close within 2.9% to that inverted with the NUPSD and the Miki

model. The tortuosity inverted with the JCAL model is 8.5% higher than that estimated with Berryman's model. Umnova's model significantly overpredicts the other estimates.

The JCAL model provides the most accurate estimate of the flow resistivity for this medium. It is accurate within 6%. The Miki model and the NUPSD model overestimate it by 23% and underestimate by 18%, respectively. Umnova's model and the KC model underpredict this parameter significantly, whereas the RGPZ model significantly overpredicts it.

We have found no published data on the thermal flow resistivity, median pore size, viscous and thermal characteristic lengths for these sands. We have no equipment to measure these parameters reliably. The values of the thermal flow resistivity inverted with the NUPSD and JCAL models seem plausible, although the JCAL model suggests a thermal flow resisitivty (10580 Pa s m^{-2}) which is suspiciously close to that of the viscous flow resistivity (11610 Pa s m^{-2}). This is unusual for a granular media in which the pore shape varies in a complex manner. The values for the viscous and thermal characteristic lengths inverted with the NUPSD model are plausible, but those inverted with the JCAL model appear on a centimeter scale and do not make physical sense. The viscous characteristic length predicted with the RGPZ model is within 13% from that inverted with the NUPSD model. Umnova's model predicts a much higher value for this parameter which is still plausible.

4.4. Sample 4: silica sand fraction B

The bottom part of Figure 4 presents an example of the comparison between the measured and predicted spectra for the complex reflection coefficient of an 80 mm hard-backed layer of silica sand fraction B. The discrepancy between the three models and measured data is

Table 5: A summary of the values of non-acoustical parameters for Sample D - (silica sand fraction B) measured, inverted acoustically and predicted non-acoustically.

Model	ϕ	α_∞	σ Pa s m^{-2}	σ' Pa s m^{-2}	$\bar{s}$ μm	$\sigma_{\bar{s}}$ φ-units	Λ μm	Λ' μm
Measured	0.380	-	35380	-	-	-	-	-
	-	-	$\pm$137	-	-	-	-	-
NUPSD	0.370	2.25	35450	4950	296	0.625	174	414
	$\pm$0.05	$\pm$0.8	$\pm$ 2767	$\pm$5105	$\pm$90	$\pm$0.2	$\pm$19	$\pm$172
JCAL	0.372	3.19	36600	13500	-	-	18666	155890
	$\pm$0.02	$\pm$0.3	$\pm$1956	$\pm$5276	-	-	$\pm$3100	$\pm$72912
Miki	0.367	2.16	30900	-	167	-	-	-
	$\pm$0.02	$\pm$0.2	$\pm$2536	-	-	-	-	-
Umnova	-	2.50	27700	-	-	-	176	-
Berryman	-	1.82	-	-	-	-	-	-
RGPZ	-	-	146700	-	-	-	91	-
KC	-	-	28800	-	-	-	91	-

relatively large. Table 5 presents a summary of the non-acoustical parameters which were inverted using the three models for the acoustical properties of porous media and analytical models detailed in section 2. This is a mix of relatively small particles (890 μm) with a relatively high viscous flow resistivity (35380 Pa s m^{-2}).

Despite a relatively poor agreement between the predicted and measured reflection coefficient spectra, the three acoustical models provide a rather accurate estimate of the porosity within 3.5% of the measured value. The Miki model and the NUPSD model invert similar tortuosity values which are within 4%. These estimates compare with 10% with the tortuosity predicted by Umnova's model.

The flow resistivity of this medium is also inverted relatively accurately with the three acoustical models. The NUPSD and JCAL model are accurate within 3.5% whereas the Miki model is accurate within 15% which is still a close estimate given the material pore

complexity.

The estimated values for the thermal flow resistivity, median pore size and standard deviation in the pore size are all plausible and physically realistic. However, the viscous and thermal characteristic lengths inverted with the JCAL model appear physically unrealistic. Obviously, these estimates are too large to make any physical sense. One problem with the JCAL model is that it is based on six non-acoustical parameters which are not independent of each other [18]. Therefore, the problem of minimisation is probably insensitive to some of these parameters which results in the inversion yielding physically unrealistic values.

5. Conclusions

The acoustical properties of four samples of unconsolidated, unsaturated granular media have been measured using a standard impedance tube setup. These acoustical data have been supplemented with the flow resistivity and porosity data which were measured non-acoustically. The NUPSD[18], JCAL[27] and Miki's[20] models have been used to invert the non-acoustical parameters of these media via an optimisation algorithm. Some of these non-acoustical parameters have been estimated using Berryman's [23], Umnova's [22], KC [24] and RGPZ [9] analytical models. An important outcome of this work is a better understanding of the accuracy of popular models to predict or invert key parameters of porous media which can be of interest in areas of science and engineering other than acoustics.

The results suggest that it is possible to estimate the porosity of these media from the available acoustical data with an accuracy of better than 10%. Given the fact that the porosity of a granular medium can vary from 26% (triclinic packing) to 48% (cubic packing), i.e. by around $\pm 25\%$, this is a relatively accurate result. In some cases, e.g. for silica sand

fraction A, the porosity estimate from the acoustic data with the Miki model was 0.1%, which is impressive given the fact that this model is empirical and depends on three parameters only.

The estimation of the flow resistivity via the parameter inversion process has been less accurate particularly for 5 mm glass beads. For this medium the flow resistivity values inverted with the JCAL and the Miki models have been underestimated by 71% and 52%, respectively. The accuracy of this estimation with the NUPSD model has been within 3.5%. We note that the measured flow resistivity for this medium is relatively low ($\sigma = 1750$ Pa s m^{-2}). The best overall accuracy for this parameter estimation of better than 15% has been achieved for silica sand fraction B. This is a relatively accurate estimation given the fact that the agreement between the measured and predicted reflection coefficient spectra for this material sample is relatively poor (see Figure 4). The estimation of the flow resistivity for these granular media with the analytical models seems problematic. The KC model can provide the most accurate estimate, e.g. within 2% for 2 mm glass beads, but this model is too sensitive to the measured porosity value, ϕ, i.e. the material compaction state. Therefore, it has been found to deviate from the measured data by up to 71% in the case of the other media studied in this work. A similar observation can be made about the accuracy of the RGPZ model which depends too much on the choice of the cementation exponent, m. The equation of Umnova for the flow resistivity (permeability) is rather sensitive to the porosity, ϕ, and tends to consistently underpredict the flow resistivity by up to 80%.

The acoustically estimated viscous and thermal characteristic lengths for glass beads agreed within 22% with the measured values. The acoustically estimated viscous characteristic lengths for silica sands made with the NUPSD, Umnova's and RGPZ models make

physical sense, but there is no data to quantify estimation errors. Similar comments can be made about the values of the thermal characteristic length estimated with the NUPSD model. The equation for the viscous characteristic length given by Umnova (Eq. (2)) is too sensitive to the porosity, ϕ. The equation for the viscous characteristic length in the RGPZ model is too sensitive to the cementation exponent, m. Therefore, the values of Λ predicted with these two equations for glass beads and sands seem to vary considerably from the measured data or inverted values if the values of ϕ and m have not been accurately measured and / or selected. The viscous and thermal characteristic lengths for these sands made with the JCAL model seem physically unrealistic. This can be attributed to the fact that the JCAL model is based on six non-acoustical parameters which are not independent (see eqs. (18)-(20)). Some of these parameters, e.g. flow resistivity, σ, porosity, ϕ, and tortuosity, α_∞, are likely to dominate in the adopted optimisation algorithm, whereas the optimisation can be insensitive to some other parameters, e.g. Λ and Λ'. The rank of the design vector, $\boldsymbol{x}$ in Eq. (27) increases with a rising number of parameters. This can lead to some ambiguity in the inverted parameter values. In this sense, the parameter inversion with a prediction model which requires a smaller number of non-acoustical parameters can appear to be a more attractive and stable method of granular media characterisation.

The main novelty of this work is in quantifying the discrepancy between the values of key non-acoustical parameters of granular media which were measured and estimated acoustically and non-acoustically. This work paves the way for acoustical characterisation of granular media with a relatively inexpensive laboratory setup and a standard optimisation algorithm which are quick and relatively accurate.

6. Acknowledgements

The authors are grateful to the UK's Engineering and Physical Sciences Research Council (Grant EP/R005001/1, UK Acoustics Network) for partial support of this work. The authors are also grateful to Dr. Alistair Hurrel and Miss Hasina Begum for help with some laboratory experiments in Sheffield.

References

[1] A. Revil, N. Florsch, Determination of permeability from spectral induced polarization in granular media, Geophysical Journal International 181 (3) (2010) 1480–1498. doi:10.1111/j.1365-246X.2010.04573.x.

[2] P. Glé, E. Gourdon, L. Arnaud, K. V. Horoshenkov, A. Khan, The effect of particle shape and size distribution on the acoustical properties of mixtures of hemp particles, The Journal of the Acoustical Society of America 134 (6) (2013) 4698–4709. doi:https://doi.org/10.1121/1.4824931.

[3] K. V. Horoshenkov, A review of acoustical methods for porous material characterisation, Int. J. Acoust. Vib 22 (2017) 92–103. doi:https://doi.org/10.20855/ijav.2017.22.1455.

[4] S. Brunauer, P. H. Emmett, E. Teller, Adsorption of gases in multimolecular layers, Journal of the American Chemical Society 60 (2) (1938) 309–319. doi:10.1021/ja01269a023.

[5] M. A. Klatt, Morphometry of random spatial structures in physics, Doctoral Thesis FAU University Press (Jan. 2016).

[6] S. Torquato, Random heterogeneous materials: microstructure and macroscopic properties, Vol. 16, Springer Science & Business Media, 2013.

[7] A. S. Clarke, H. Jónsson, Structural changes accompanying densification of random hard-sphere packings, Physical Review E 47 (6) (1993) 3975. doi:https://doi.org/10.1103/PhysRevE.47.3975.

[8] S. Torquato, F. H. Stillinger, New conjectural lower bounds on the optimal density of sphere packings, Experimental Mathematics 15 (3) (2006) 307–331. doi:https://doi.org/10.1080/10586458.2006.10128964.

[9] P. Glover, I. Zadjali, K. Frew, Permeability prediction from MICP and NMR data using an electrokinetic approach, Geophysics 71 (4) (2006) F49–F60.

[10] J. F. Allard, M. Henry, J. Tizianel, L. Kelders, W. Lauriks, Sound propagation in air-saturated random packings of beads, The Journal of the Acoustical Society of America 104 (4) (1998) 2004–2007. doi:https://doi.org/10.1121/1.423766.

[11] Z. E. A. Fellah, C. Depollier, M. Fellah, Application of fractional calculus to the sound waves propagation in rigid porous materials: Validation via ultrasonic measurements, ACTA Acustica United with Acustica 88 (2002) 34–39.

[12] Z. E. A. Fellah, S. Berger, W. Lauriks, C. Depollier, P. Trompette, J. Y. Chapelon, Ultrasonic measurement of the porosity and tortuosity of air-saturated random packings

of beads, Journal of Applied Physics 93 (11) (2003) 9352–9359. doi:https://doi.org/10.1063/1.1572191.

[13] P. Leclaire, O. Umnova, K. V. Horoshenkov, L. Maillet, Porosity measurement by comparison of air volumes, Review of Scientific Instruments 74 (3) (2003) 1366–1370. doi:https://doi.org/10.1063/1.1542666.

[14] M. A. Biot, Theory of propagation of elastic waves in a fluid-saturated porous solid. ii. Higher frequency range, The Journal of the Acoustical Society of America 28 (2) (1956) 179–191. doi:https://doi.org/10.1121/1.1908241.

[15] http://apmr.matelys.com/PropagationModels/MotionlessSkeleton/JohnsonChampouxAllardModel.html. doi:http://apmr.matelys.com/.

[16] D. L. Johnson, J. Koplik, R. Dashen, Theory of dynamic permeability and tortuosity in fluid-saturated porous media, Journal of Fluid Mechanics 176 (1987) 379–402. doi:https://doi.org/10.1017/S0022112087000727.

[17] J. Allard, N. Atalla, Propagation of sound in porous media: modelling sound absorbing materials, John Wiley & Sons, 2009.

[18] K. V. Horoshenkov, A. Hurrell, J.-P. Groby, A three-parameter analytical model for the acoustical properties of porous media, The Journal of the Acoustical Society of America 145 (4) (2019) 2512–2517. doi:https://doi.org/10.1121/1.5098778.

[19] Y. Champoux, J.-F. Allard, Dynamic tortuosity and bulk modulus in air-saturated porous media, Journal of Applied Physics 70 (4) (1991) 1975–1979. doi:https://doi.org/10.1063/1.349482.

[20] Y. Miki, Acoustical properties of porous materials-generalizations of empirical models, Journal of the Acoustical Society of Japan (E) 11 (1) (1990) 25–28. doi:https://doi.org/10.1250/ast.11.25.

[21] K. V. Horoshenkov, J.-P. Groby, O. Dazel, Asymptotic limits of some models for sound propagation in porous media and the assignment of the pore characteristic lengths, The Journal of the Acoustical Society of America 139 (5) (2016) 2463–2474. doi:https://doi.org/10.1121/1.4947540.

[22] O. Umnova, K. Attenborough, K. M. Li, Cell model calculations of dynamic drag parameters in packings of spheres, The Journal of the Acoustical Society of America 107 (6) (2000) 3113–3119. doi:https://doi.org/10.1121/1.429340.

[23] J. G. Berryman, Confirmation of Biot's theory, Applied Physics Letters 37 (4) (1980) 382–384. doi:https://doi.org/10.1063/1.91951.

[24] P. Carman, Flow of gases through porous media, Butterworths, London (1956).

[25] B. Yavari, A. Bedford, Comparison of numerical calculations of two Biot coefficients with analytical solutions, The Journal of the Acoustical Society of America 90 (2) (1991) 985–990. doi:https://doi.org/10.1121/1.401912.

[26] R. D. Stoll, Sediment acoustics (lecture notes in earth sciences), Berlin, Germany: Springer-Verlag (1989).

[27] J.-F. Allard, Y. Champoux, New empirical equations for sound propagation in rigid frame fibrous materials, The Journal of the Acoustical Society of America 91 (6) (1992) 3346–3353. doi:https://doi.org/10.1121/1.402824.

[28] A. Revil, L. Cathles, Permeability of shaly sands, Water Resources Research 35 (3) (1999) 651–662. doi:https://doi.org/10.1029/98WR02700.

[29] K. V. Horoshenkov, K. Attenborough, S. N. Chandler-Wilde, Padé approximants for the acoustical properties of rigid frame porous media with pore size distributions, The Journal of the Acoustical Society of America 104 (3) (1998) 1198–1209. doi:https://doi.org/10.1121/1.424328.

[30] R. J. Wakeman, Packing densities of particles with log-normal size distributions, Powder Technology 11 (3) (1975) 297–299. doi:https://doi.org/10.1016/0032-5910(75)80055-6.

[31] Y. Atalla, R. Panneton, Inverse acoustical characterization of open cell porous media using impedance tube measurements, Canadian Acoustics 33 (1) (2005) 11–24.

[32] ISO 10534-2:1998. Determination of sound absorption coefficient and impedance in impedance tubes, Part 2: Transfer-function method.
URL https://www.iso.org/standard/22851.html

[33] ISO 9053:1991 Acoustics – Materials for acoustical applications – Determination of airflow resistance.
URL https://www.iso.org/standard/16622.html

[34] Supplementary data including impedance tube files and Matlab code.
URL https://drive.google.com/drive/folders/1UMFp_ICYded4zw-i9nRhVrrhbgrnUkG_?usp=sharing[accessedon28/06/2021]

[35] P. Glover, E. Walker, Grain-size to effective pore-size transformation derived from electrokinetic theory, Geophysics 74 (1) (2009) E17–E29.

[36] P. Leclaire, M. Swift, K. Horoshenkov, Determining the specific area of porous acoustic materials from water extraction data, Journal of Applied Physics 84 (12) (1998) 6886–6890.

[37] K. Horoshenkov, M. Swift, The acoustic properties of granular materials with pore size distribution close to log-normal, The Journal of the Acoustical Society of America 110 (5) (2001) 2371–2378. doi:https://doi.org/10.1121/1.1408312.